


# Silver Nanoparticles Cause Neural and Vascular Disruption by Affecting Key Neuroactive Ligand-Receptor Interaction and VEGF Signaling Pathways

Chunjiao Lu\*, Yi Liu\*, Yao Liu, Guanhua Kou, Yang Chen, Xuwei Wu, Yuhang Lv, Jiahao Cai, Renyuan Chen, Juanjuan Luo, Xiaojun Yang 

Guangdong Provincial Key Laboratory of Infectious Disease and Molecular Immunopathology, Shantou University Medical College, Shantou, 515041, People's Republic of China

\*These authors contributed equally to this work

Correspondence: Juanjuan Luo; Xiaojun Yang, Guangdong Provincial Key Laboratory of Infectious Disease and Molecular Immunopathology, Shantou University Medical College, Shantou, 515041, People's Republic of China, Tel +86-754-88900236, Fax +86-754-88900276, Email [lujj770@163.com](mailto:lujj770@163.com); [yangx@stu.edu.cn](mailto:yangx@stu.edu.cn)

**Introduction:** Silver nanoparticles (AgNP) are widely used as coating materials. However, the potential risks of AgNP to human health, especially for neural and vascular systems, are still poorly understood.

**Methods:** The vascular and neurotoxicity of various concentrations of AgNP in zebrafish were examined using fluorescence microscopy. In addition, Illumina high-throughput global transcriptome analysis was performed to explore the transcriptome profiles of zebrafish embryos after exposure to AgNP. Kyoto Encyclopedia of Genes and Genomes (KEGG) enrichment analyses were conducted to elucidate the top 3000 differentially expressed genes (DEGs) between AgNP-exposed and control groups.

**Results:** We systematically investigated the neural and vascular developmental toxicities of AgNP exposure in zebrafish. The results demonstrated that AgNP exposure could cause neurodevelopmental anomalies, including a small-eye phenotype, neuronal morphology defects, and inhibition of athletic abilities. In addition, we found that AgNP exposure induces angiogenesis malformation in zebrafish embryos. Further RNA-seq revealed that DEGs were mainly enriched in the neuroactive ligand-receptor interaction and vascular endothelial growth factor (Vegf) signaling pathways in AgNP-treated zebrafish embryos. Specifically, the mRNA levels of the neuroactive ligand-receptor interaction pathway and Vegf signaling pathway-related genes, including *si:ch73-55i23.1*, *nfatc2a*, *prkeg*, *si:ch211-132p1.2*, *lepa*, *mchr1b*, *pla2g4aa*, *rac1b*, *p2ry6*, *adrb2*, *chrnl1*, and *chrm1b*, were significantly regulated in AgNP-treated zebrafish embryos.

**Conclusion:** Our findings indicate that AgNP exposure transcriptionally induces developmental toxicity in neural and vascular development by disturbing neuroactive ligand-receptor interactions and the Vegf signaling pathway in zebrafish embryos.

**Keywords:** silver nanoparticles, neurological development, vascular development, developmental toxicity, zebrafish

## Introduction

Silver nanoparticles (AgNP) are widely used in commercial products, including antimicrobial agents, laundry additives, paints, textiles, and personal care products, and are increasingly detected in aquatic ecosystems.<sup>1</sup> AgNP products can also release monovalent silver, silver ions and nanoparticles into aquatic systems, which negatively impacts organisms.<sup>2</sup> Previous studies have indicated that silver particles can cross the human placental barrier and accumulate in the fetus,<sup>3</sup> and cross the chorionic pores/membranes in fish embryos,<sup>4-7</sup> suggesting that AgNP can cause serious effects in aquatic ecosystems due to their potential adverse impact on aquatic species.<sup>1</sup>

Previous reports have illustrated AgNP-induced developmental toxicities in various aquatic organisms.<sup>8–10</sup> Exposure to > 500 mg/kg AgNP can lead to death in the freshwater fish *Labeo rohita*, whereas approximately 25 mg/kg AgNP treatment affects hematological parameters and enzymatic activities.<sup>11</sup> Powers et al reported that AgNP treatment caused developmental neurotoxicity that affects the neural behavior in zebrafish.<sup>12</sup> After entering the zebrafish brain, AgNP causes apoptosis in the head region and alters development-related gene expression levels.<sup>13,14</sup> AgNP treatment can also lead to other phenotypic disruptions in zebrafish embryos, including small heads with hypoplastic hindbrain and microphthalmos.<sup>15</sup> In addition, a previous study showed that AgNP exposure delays zebrafish embryonic vascular development,<sup>5</sup> suggesting that AgNP can induce vascular toxicity in vascular development in zebrafish embryos. However, the potential regulatory mechanisms underlying AgNP-induced neural and vascular developmental toxicity are still not fully understood.

As an animal model for studying environmental toxicity, zebrafish have unique advantages, including low cost, small size, and strong reproductive abilities. Importantly, fluorescent-labeled transgenic zebrafish can be used to easily visualize the development of nervous and vascular systems because of the transparency advantage of zebrafish embryos.<sup>16</sup> The present study attempted to clarify the potential neural and vascular toxicity of AgNP in vivo by using the unique features of the zebrafish model. Specifically, the hypothesis was raised that AgNPs could induce the developmental disruption of neural and vascular systems by perturbing the related signaling pathway in neural and vascular development in zebrafish embryos. In this context, we dynamically determined the effect of AgNP on neural and vascular development in AgNP-treated zebrafish embryos during early-stage development. Furthermore, the morphology of neural and vascular development and behavioral phenotypes were examined in zebrafish embryos after AgNP treatment at various concentrations. After that, to elucidate the potential mechanism of AgNP-induced developmental disruption, global transcriptome analysis was performed to identify the downstream regulatory signaling pathway in this process. Specifically, neuroactive ligand-receptor interaction and vascular endothelial growth factor (Vegf) signaling pathways were identified and confirmed using quantitative reverse transcription-polymerase chain reaction (qRT-PCR) in AgNPs-treated zebrafish embryos. Moreover, we found that some key regulatory factors of neuroactive ligand-receptor interactions and Vegf signaling pathways were significantly regulated after AgNP treatment in zebrafish. Thus, our results indicate that AgNP induced neural and vascular developmental toxicities by disturbing neuroactive ligand-receptor interaction and VEGF signaling pathways in vivo and in vitro.

## Materials and Methods

### Ethics Statement

This study was performed in strict accordance with the recommendations of the Guide for the Care and Use of Laboratory Animals of the Shantou University Medical College. The study protocol was approved by the Shantou University Medical College Animal Committee.

### The Preparation and Examination of AgNP

AgNP powder (CAS No. 7440–22–4) was purchased from Sigma-Aldrich (Merck, Germany) and suspended in ultrapure water (Millipore, Sigma-Aldrich). An AgNP stock solution (100 mg/L) was prepared for 50 min at 50 W/L, 40 kHz after sonicating. The morphology of AgNP was characterized by transmission electron microscope (TEM) according to the previously described.<sup>17</sup> The exposure solutions of AgNP were prepared every 24 h to maintain fresh and consistent levels of exposure.

### Zebrafish Maintenance and AgNP Treatment

Wild-type (WT) and *Tg(flk:eGFP)* transgenic zebrafish lines were obtained from China Zebrafish Resource Center (Wuhan, China). The transgenic *Tg(Hb9:eGFP)* fish line was provided by Professor Yajun Wang (Sichuan University, China). All fish were maintained according to the standard husbandry protocol at 28 °C with a 14 h light/10 h dark cycle and fed twice daily with fresh brine shrimp.<sup>18</sup> For breeding, six adult fish (three males and three females) were bred to

produce embryos in the breeding tank on the day before breeding. The next morning, the embryos were collected by siphoning the bottom of the breeding tank and temporarily maintained in E<sub>3</sub> embryonic medium.

For AgNP exposure, healthy zebrafish embryos (4 h post-fertilization [hpf]) were selected and treated with AgNP at various concentrations (0, 1, 2, and 4 mg/L) at 4 hpf for 24–96 h. The dose ranges were designed according to the preliminary experiments by determining the toxicological effects of AgNP with an LC<sub>50</sub> assay in 4 hpf fish embryos after 96 h of exposure.<sup>17</sup>

## Inductively Coupled Plasma Mass Spectrometry (ICP-MS)

The metal ion detection in tissues was determined according to a previously described protocol.<sup>19</sup> Briefly, zebrafish embryos treated with different concentrations of AgNP for 72 h (n = 100 for each group) were washed with ultrapure water (Milli-Q, Millipore Inc., Bedford, MA) before storing in the ultra-low temperature freezer for the following experiments. Before digestion, all samples were transferred to a Teflon tube and dried in an oven at 80 °C for 8 h. After that, the sample was digested with 250 µL 65% nitric acid (Merk, Darmstadt, Germany) in a water bath at 80 °C for 1 h, and then diluted with 3% nitric acid, and analyzed by using ICP-MS (Agilent 7900, Agilent Technologies, Santa Clara, CA). Ag concentrations were calculated with a 9-point calibration curve within the concentration ranges after continuously diluting a standard solution with 3% nitric acid. Three replicates were set for control and experimental groups.

## Cell Culture and AgNP Treatment

Human umbilical vein endothelial cells (HUVECs) were obtained from American Type Culture Collection (ATCC, Manassas, VA) and seeded in supplemented endothelial cell growth medium (Gibco, Thermo Fisher Scientific, Waltham, MA) in a humidified incubator with 5% CO<sub>2</sub> atmosphere at 37 °C. To analyze the AgNP exposure in HUVECs, we seeded cells in 6-well plates (1×10<sup>5</sup> cells/well) and cultured them at 37 °C for 12 h. After that, the cells were exposed to a fresh medium containing various concentrations of AgNP (0, 1, 2, and 4 mg/L), and the cells were incubated at 37 °C for 72 h. All experiments were repeated, at least in triplicate.

## The Determination of Neuronal Network and Vasculatures in AgNP-Treated Zebrafish

For all treatments, 0.003% phenylthiourea (PTU) was used to eliminate pigmentation in zebrafish embryos. The fluorescence-labeled neuronal network and vasculature were determined in *Tg(Hb9:eGFP)* and *Tg(flk:eGFP)* transgenic zebrafish embryos with or without 72-h of AgNP exposure at various concentrations using a fluorescence microscope (Zeiss Axio Imager, ZEISS, Germany). Images were acquired using a Zeiss Axio Imager and analyzed using ImageJ software (National Institutes of Health, Bethesda, MD, USA).

To evaluate the development of motor neurons in the nervous system, we performed fluorescence microscopy to determine the fluorescence intensity of the spinal cord of neurons, the number of caudal side neurons, and the axon length of the spinal motoneuron.

For vasculature observation in AgNP-treated zebrafish embryos, images of the vasculatures, including the intersegmental vessel (ISV), subintestinal venous plexus (SIVP), and vessels of brain tissue in the different groups, were analyzed using ImageJ software. After that, the number of abnormal ISV, areas of SIVP, and fluorescence intensity of vessels in brain tissues were determined in different treatment groups using a fluorescence microscope.

## Behavioral Tests

The motor capabilities of the larvae in the different groups were evaluated using a Zebralab Video tracking system (ViewPoint Life Science, France). After 96 h of AgNP exposure, zebrafish larvae of the different groups were transferred to a 24-well plate (one larva in each well). The swim path of each larva was recorded using a video camera for over 30 min through a 5-minute-cycle light-to-dark photoperiod stimulation. After that, quantified data of the trajectory distances of zebrafish larvae from different groups (n = 24 for each group) were analyzed using the Zebralab Video Tracking system.

## Wound Healing and Tumor Formation Angiogenesis Assay

After exposure to AgNP for 72 h, HUVECs were collected for wound healing and tube formation assays. Different groups of HUVECs, with or without AgNP treatment, were seeded in 24-well plates. After removing the cell culture medium and scratching the cell layer with a 200  $\mu$ L pipette tip, the cells were photographed at different post-scratch time points (0 and 18 h) using a phase-contrast microscope. Wound width was measured using the ImageJ software.

Matrigel (BD Bioscience, San Jose, CA, USA) was melted into a yellow gelatinous liquid at 4 °C overnight for the tube formation angiogenesis assay. The cooled, gelatinous liquid was promptly added to a 96-well plate using a prechilled micropipette and incubated at 37 °C for 30 min for solidification. The cell suspensions ( $3 \times 10^4$  cells) from different groups were seeded in solidified Matrigel and incubated with 2% FBS growth factor-free Endopan medium for 3 h. Images were captured using a Zeiss Axio Imager and analyzed using ImageJ software.

## Global Transcriptome Analysis

After 72 h of AgNP exposure, total RNA from different groups of zebrafish embryos was extracted using the TRIzol™ reagent (Invitrogen, Thermo Fisher Scientific). Transcriptome sequencing was performed by the BGI Company (Shenzhen, China) to investigate the differentially expressed genes (DEGs) of AgNP-treated and normal control groups. The top 3000 most variable DEGs were selected and analyzed for functional enrichment. Kyoto Encyclopedia of Genes and Genomes (KEGG) signaling pathway analyses and further identification of potential functions of DEGs of neuroactive ligand-receptor interaction and Vegf signaling pathways in zebrafish after AgNP exposure were analyzed using KOBAS 3.0 software.<sup>20</sup>

## RNA Extraction, cDNA Synthesis, and RT-qPCR

Total RNA was extracted from zebrafish embryos for 72 h of AgNP exposure using the TRIzol™ reagent. The different RNA samples were dissolved in RNase-free water, reverse-transcriptionally synthesized cDNA, and PCR was performed as described previously.<sup>21,22</sup> The housekeeping gene  $\beta$ -actin was chosen as the internal control.<sup>23</sup> The expression levels of target genes were normalized to  $\beta$ -actin using the  $2^{-\Delta\Delta CT}$  method. The specific primers for the targeted genes were designed using Primer 5.0 software and are shown in Table 1.

**Table 1** Primer Sequences Used for qPCR

Genes	Sequences of the Forward Primers (5'–3')	Sequences of the Reverse Primers (5'–3')
<i><math>\beta</math>-actin</i>	CCCAGACATCAGGGAGTGAT	TCTCTGTTGGCTTTGGGATT
<i>kdr</i>	TCCCCTTACCCTGGCTTACA	GTGGGACTCTGGTTTGAGGG
<i>zgc:171775</i>	CACCTGAGTGACCGTGAACA	CCCAACAGGCTTGAGAGAGG
<i>nfatc2a</i>	AAAGCCCTGAGTCTCCGACAT	ACTGGAGTATCAAGAGCGGC
<i>si:ch73-55i23.1</i>	TGCTGACGGATCTTACCGAC	GCACCGAGAAGTAGGGTGAG
<i>mapk1</i>	CAAATAGACCCATCTTCCC	TTCCTCCACCTCAATCCTC
<i>pla2g4aa</i>	GGAGCATTTGGGGATTTA	CCATTTGTGCCACTTTGA
<i>prkcg</i>	TACTTTTTTCAGTGCGGGGCA	CTGGATCAGGCACAGGGATG
<i>lepa</i>	AAGGAAAGCTGCAAATTGAAGAG	AAGTTCACCATGGGTCACGG
<i>mchr1b</i>	CAGTGTGGATGTATGCGGGT	GAGGCGCCCAACAAATGAAG
<i>si:ch211-132p1.2</i>	TTTGCCCATGCGGTTAGAGT	AGAGCCTCCCATGACCTCTT
<i>chrmb1</i>	TTCTACTTGCCACCCGA	TGAGCACCACGACACTG
<i>cckar</i>	TGCTCATGCTGCCTTATCCC	AGTTTGGATTTGGGGTGGCT
<i>p2ry6</i>	ATACGGCATCGCTTTGACCT	ACGGCAAAAAGCTAATGGCG
<i>adrb2a</i>	TTACAGCCGTGTGTTCCAGG	CACCGAGCCCTTGGGAATAA
<i>chrmlb</i>	AAGCGAACTCCAAAACGGC	ATCGCCGTGCCGTATGTTAT
<i>rac1b</i>	GTCGCTCGTTAGAGGGGTTT	CCAGATTCACCGGTTTCCCA
<i>sstr2a</i>	GTCATCCTACGCTACGCCAA	AGAAGCGAGAGCTGTATGGC
<i>lpar4</i>	TGCATCAGTGTGGATCGCTT	GAGTTGCTGTTGACGCAAG

## Quantification and Statistical Analysis

Significant differences were analyzed by one-way analysis of variance (ANOVA) and Tukey's multiple range tests using GraphPad Prism Version 8.0 (GraphPad Software, San Diego, CA, USA) and presented as the means  $\pm$  standard error (SEM). Statistical significance was set at  $P < 0.05$ .

## Results

### Quantification of Ag Uptake in Zebrafish

The sizes of AgNPs were characterized using TEM according to our previously described report.<sup>17</sup> The Ag uptake in zebrafish embryos treated with or without AgNPs at different concentrations was determined by ICP-MS. As shown in Table 2, the Ag content of zebrafish exposed to different concentrations for 72 h was detected. The results indicated that the content of Ag in the control samples was approximately  $2.5 \times 10^{-3}$  ng in each embryo ( $n = 100$  for each group). However, in AgNPs-treated groups, the contents of Ag were averagely from  $6.0 \times 10^{-2}$  to  $2.0 \times 10^{-1}$  ng in each embryo ( $n = 100$  for each group), indicating that Ag content was in a dose-dependent manner after AgNPs treatment at different concentrations in zebrafish embryos.

### AgNP Exposure Impairs Neural Development in Zebrafish

Then, the morphological phenotypes of zebrafish embryos after AgNP exposure at various concentrations were measured. As shown in Figure 1A, the significant "small eye" phenotype was detected in AgNP-treated zebrafish embryos after 48 and 72 h of exposure (red frames; Figure A). Furthermore, compared with the untreated group, AgNP exposure, especially at higher concentrations (2 and 4 mg/L), resulted in significant abnormality of small eye size after 48 and 72 h of exposure in a dose-dependent manner in zebrafish embryos ( $P < 0.01$ ; Figure 1B and C), especially in the higher concentration group (4 mg/L;  $P < 0.001$ ), suggesting that AgNP exposure morphologically affects the neural system in zebrafish.

To explore the toxic effects of AgNP on the neural system during development, the transgenic zebrafish line *Tg(Hb9:eGFP)*, which labeled neuronal cells with enhanced green fluorescent protein (eGFP) in zebrafish, was used to dynamically visualize neural development in AgNP-treated zebrafish at various concentrations (Figure 2A). Unlike the intact eGFP-labeled neuronal network in the untreated control group, the results indicated that the neuronal network showed a downward trend in the higher concentration groups after 72 h of AgNP exposure in zebrafish embryos by determining the fluorescence intensity of eGFP-labeled-spinal cord motor neurons (red arrowheads; Figure 2A and B). Notably, the integrity of the neuronal network was disrupted after 72 h of AgNP exposure in zebrafish embryos (red broken frames; Figure 2A). Furthermore, quantitative analyses demonstrated that the number of caudal side neurons (Figure 2C) and the length of axons (yellow arrowheads and asterisks; Figure 2A and D) were significantly reduced in a dose-dependent manner in zebrafish embryos after 72 h of AgNP exposure, suggesting that AgNP can impair the neural system in zebrafish at an early developmental stage.

In general, the locomotor behavior of zebrafish plays a crucial role in neural development, and disruption of the neural system is usually accompanied by motility dysfunction. We then performed behavioral tests to evaluate the potential effects of AgNP exposure on neural development in zebrafish (Figure 2E). After 96 h of exposure, the motor capabilities of the AgNP-treated zebrafish larvae at various concentrations were determined. The results indicated that the

**Table 2** Ag Uptake in Zebrafish Embryos with or Without AgNP Treatment at Different Concentrations

Sample	Ag	P value	LOAEL
Fishwater	0.015 $\mu$ g/L		NA
Control Fish (n=100, with 3 replicates)	0.0025 $\pm$ 0.0003 ng per fish		NA
1 mg/L Treatment Group (n=100, 3 replicates)	0.0599 $\pm$ 0.0030 ng per fish	< 0.0001****	1 mg/L
2 mg/L Treatment Group (n=100, 3 replicates)	0.0806 $\pm$ 0.0038 ng per fish	< 0.0001****	2 mg/L
4 mg/L Treatment Group (n=100, 3 replicates)	0.1994 $\pm$ 0.0098 ng per fish	< 0.0001****	4 mg/L

Note: \*\*\*\*P < 0.0001.

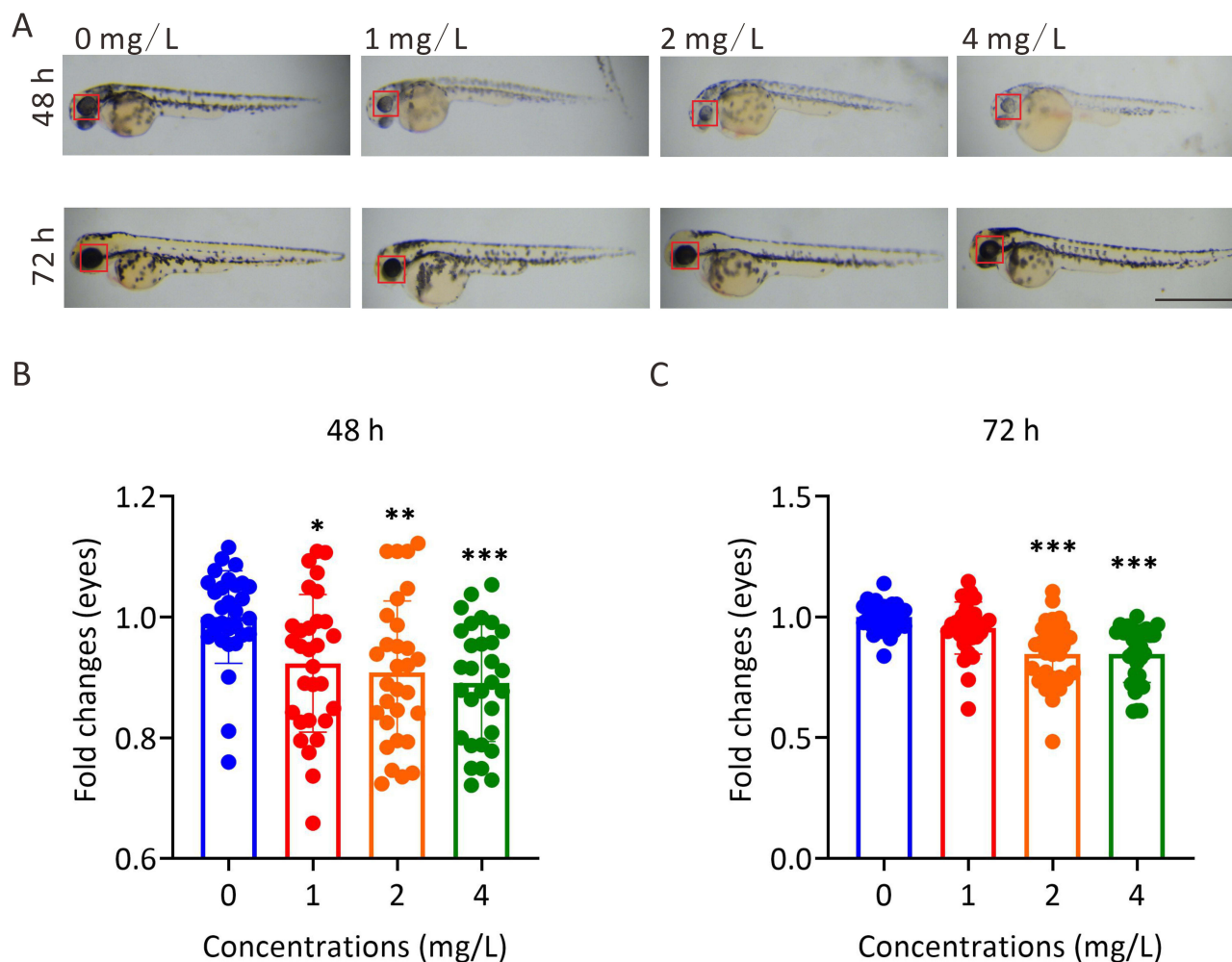


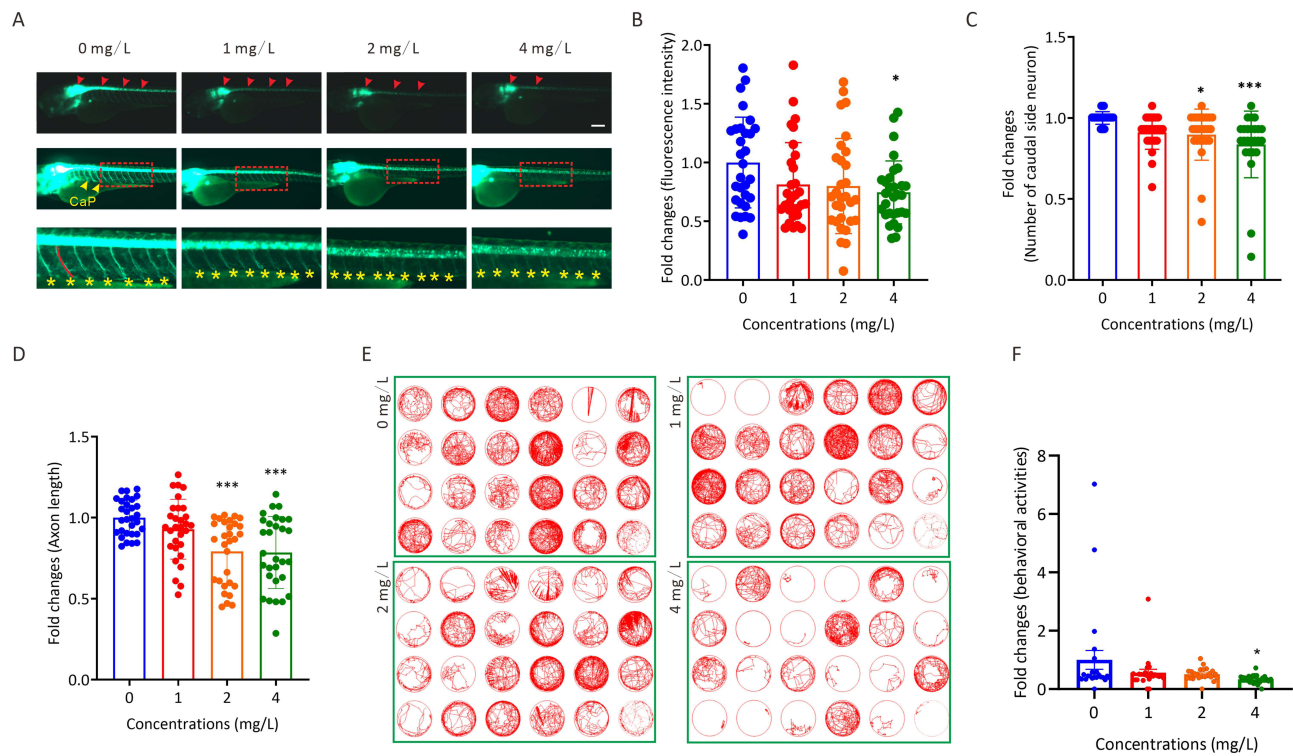
**Figure 1** The effect of AgNP treatment on eye development in zebrafish. **(A)** The morphology of zebrafish eyes after 48 and 72 h of AgNP treatment, Scale bar, 1 mm. **(B and C)** Quantification of the diameters of whole eyes of zebrafish after 48 and 72 h of AgNP treatment ( $n = 30$  for each group). Data are shown as the means  $\pm$  SEM. \* $P < 0.05$ , \*\* $P < 0.01$ , \*\*\* $P < 0.001$ . Red boxes, eye regions.

traveling distances of larvae were significantly reduced after treatment with 4 mg/L AgNP ( $P < 0.05$ ; **Figure 2F**). Therefore, the results indicate that AgNP exposure-induced behavioral toxicity may be positively correlated with the disruption of neural development at the early developmental stage in a dose-dependent manner in zebrafish larvae.

## AgNP Exposure Results in Vascular Malformation in Zebrafish

To illustrate the roles of AgNP exposure during vascular development in zebrafish embryos, the transgenic zebrafish line *Tg(flk:eGFP)*, which labeled vascular endothelial cells with an eGFP reporter in zebrafish, was used to evaluate the vascular development in zebrafish with or without AgNP treatment (**Figure 3A**). In this context, accurate vascular development of the trunk axial vessels, including the dorsal longitudinal anastomotic vessel (DLAV, white arrowheads), intersegmental vessel (ISV, asterisks), dorsal aorta (DA, red arrowheads), and posterior cardinal vein (PCV, arrows), which were labeled by fluorescence, were performed (upper panel; **Figure 3A**). The results indicated that the number of abnormal patterning of ISV spouts in randomly selected transgenic *Tg(flk:eGFP)* embryos ( $n = 9$  for each group) increased ( $P < 0.05$ ) in the higher concentration (4 mg/L) group after 72 h of AgNP exposure (**Figure 3B**).

The malformation of the vasculature of the SIVP is conventionally used as a readily discernible model to evaluate vascular malformation.<sup>24</sup> We noticed that the SIVP areas shrank (yellow broken circles, middle panel; **Figure 3A**) in 72-h AgNP-treated zebrafish embryos. Furthermore, a trend toward smaller SIVP areas was observed with the treatment of AgNP in a dose-dependent manner ( $n = 15$ ), especially in the higher concentration (4 mg/L) group ( $P < 0.001$ ;



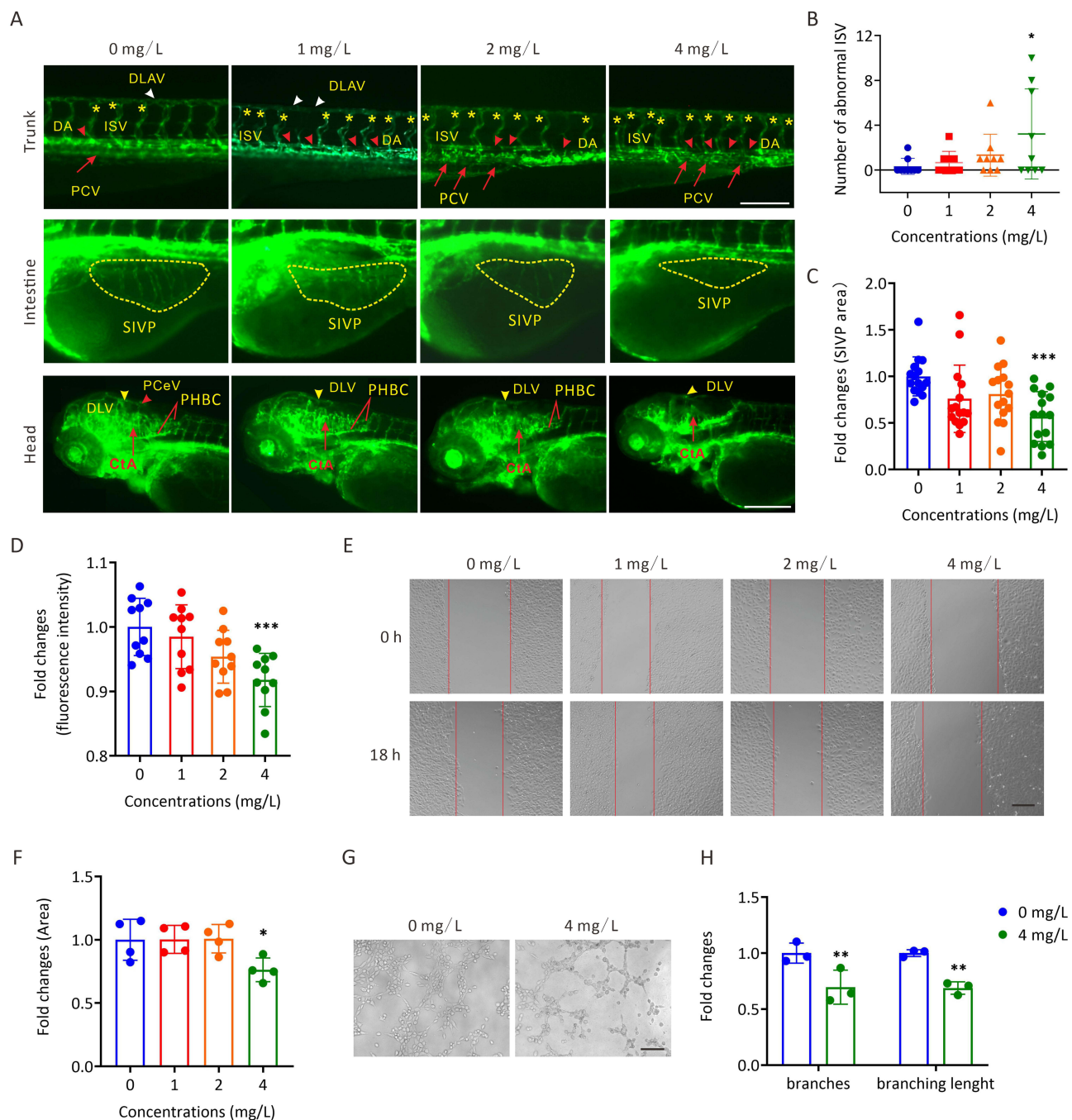
**Figure 2** The effect of AgNP treatment on neurodevelopment in zebrafish. **(A)** Neuronal morphology of zebrafish embryos after 72 h of AgNP treatment. Scale bar, 200  $\mu$ m. **(B)** Quantification of the fluorescence intensity of motor neurons in zebrafish after 72 h of AgNP treatment ( $n = 30$  for each group). **(C)** Quantification of the number of caudal side neurons in zebrafish after 72 h of AgNP treatment ( $n = 25$  for each group). **(D)** Quantification of the axon lengths of motor neurons in AgNP-treated zebrafish embryos after 72 h ( $n = 30$  for each group). **(E)** Moving track graphs of zebrafish larvae after 96 h of AgNP treatment at various concentrations. **(F)** The behavioral abilities of zebrafish larvae treated with AgNP for 96 h ( $n = 24$  for each group). Data are shown as the means  $\pm$  SEM. \* $P < 0.05$  and \*\*\* $P < 0.001$ . Red arrowheads represent spinal cord motor neurons, and yellow arrowheads or asterisks represent axons.

Figure 3C). Similar results were observed in the vasculature of the brain tissue of AgNP-treated zebrafish embryos (lower panel; Figure 3A). Furthermore, after determining the fluorescence intensities of eGFP-labeled vasculature, quantification analyses revealed that fluorescent intensities of blood vessels in the brain decreased after 72 h of AgNP exposure in a dose-dependent manner ( $n = 10$ ; Figure 3D), implying that AgNP exposure is likely to induce the malformation and/or suppression of vascular development in a dose-dependent manner, especially in higher concentration groups in zebrafish.

Further analyses were performed to elucidate the potential role of AgNP exposure in angiogenesis in vitro. The scratch wound healing assay revealed that cell migration ability was significantly reduced in HUVECs treated with 4 mg/L AgNP-treated group in HUVECs ( $P < 0.05$ ; Figure 3E and F). In addition, the tube formation assay showed that AgNP exposure could affect the angiogenic capability (Figure 3G). As shown in Figure 3H, either the number of branches or branching length was significantly lower in the AgNP-treated groups than in the control group ( $P < 0.01$ ), which is consistent with our results that AgNP exposure induces vascular malformation in zebrafish embryos.

## Identification of Downstream Signaling Pathways in AgNP-Induced Developmental Disruption in Zebrafish

To further illustrate the mechanism by which AgNP exposure impairs neural and vascular development in zebrafish embryos, RNA-seq was performed to identify the regulated downstream signaling pathways in AgNP-treated zebrafish embryos. The top 3000 DEGs in zebrafish embryos after treatment with AgNP at various concentrations (2 and 4 mg/L) were analyzed. KEGG enrichment analysis showed that several signaling pathways, including metabolic pathways, the mitogen-activated protein kinase (MAPK) signaling pathway, glycolysis/gluconeogenesis, phototransduction, fructose and mannose metabolism, and carbon metabolism, were mainly regulated in the 2 mg/L AgNP-treated group (Figure 4A). In addition, the results indicated that the DEGs were mainly enriched in the MAPK signaling pathway, AGE-RAGE



**Figure 3** The toxic effects of AgNP exposure on vascular development in zebrafish embryos and HUVECs. **(A)** Representative images of vasculatures of *Tg(flk:eGFP)* zebrafish treated with AgNP for 72 h. Scale bars, 200  $\mu$ m. **(B)** Number of abnormal ISV in zebrafish embryos after 72 h of AgNP treatment at various concentrations ( $n = 9$  for each group). **(C)** The areas of the SIVP basket in AgNP-treated zebrafish embryos after 72 h at various concentrations ( $n = 15$  for each group). **(D)** The fluorescence intensities of blood vessels in the brains of zebrafish embryos after 72 h of AgNP treatment at various concentrations ( $n = 10$  for each group). **(E and F)** The representative images and quantification of scratch migration in HUVECs with and without AgNP treatment at various concentrations (0, 1, 2, and 4 mg/L) and time points (0 and 18 h;  $n = 4$  replicates). **(G and H)** Representative images and quantification of tube formation in AgNP-treated HUVECs at various concentrations (0 and 4 mg/L;  $n = 3$  replicates) after 72 h. Data are shown as the means  $\pm$  SEM. \* $P < 0.05$ , \*\* $P < 0.01$ , and \*\*\* $P < 0.001$ . In the trunk panel are red arrowheads, DA; white arrowheads, DLAV; red arrows, PCV; asterisks, ISV. In the intestine panel, yellow broken circle, SIVP. In the head panel are yellow arrowheads, DLV; red arrowheads, PCeV; red lines, PHBC; red arrows, CtA; red arrowhead, PCeV. **Abbreviations:** DLAV, dorsal longitudinal anastomotic vessel; DLV, dorsal longitudinal vein; ISV, intersegmental vessel; PCV, posterior cardinal vein; DA, dorsal aorta; SIVP, subintestinal venous plexus; PHBC, primordial hindbrain channel; CtA, central artery; PCeV, posterior cerebral vein.

signaling pathway in diabetic complications, calcium signaling pathway, metabolic pathways, and endocytosis after exposure to AgNP at higher concentrations (4 mg/L) in zebrafish embryos (Figure 4B). Notably, both neuroactive ligand-receptor interactions and the Vegf signaling pathway, which are known as the key regulatory signals in neural and



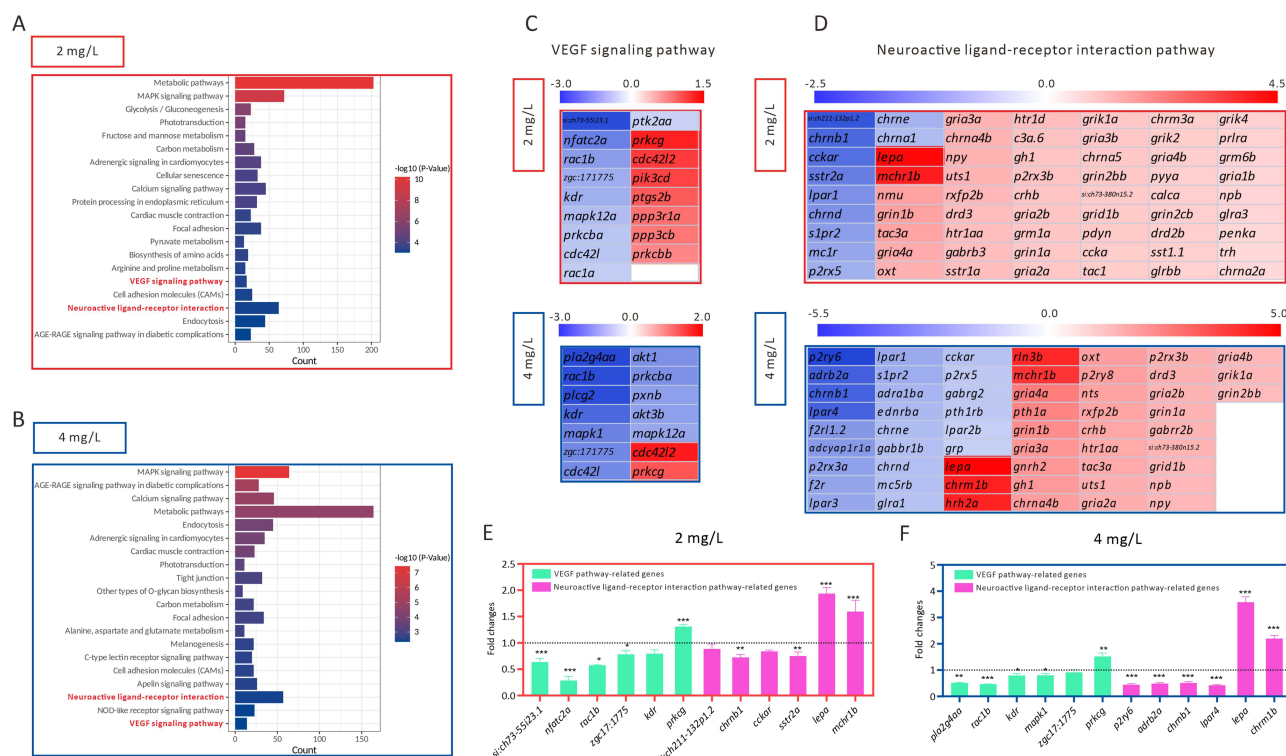


**Figure 4** The identification of downstream pathways in AgNP-induced developmental disruption in zebrafish embryos. **(A and B)** The KEGG pathway enrichment analysis of top 3000 DEGs in zebrafish embryos after 72 h of AgNP exposure at various concentrations. **(C and D)** Heat map analysis of the DEGs enriched in neuroactive ligand-receptor interaction and Vegf signaling pathways in zebrafish embryos after 72 h of AgNP exposure at various concentrations. **(E and F)** The mRNA level of neuroactive ligand-receptor interaction and Vegf pathway-related genes in zebrafish embryos after AgNP exposure at various concentrations ( $n = 3$  replicates). Data are shown as the means  $\pm$  SEM. \* $P < 0.05$ , \*\* $P < 0.01$ , and \*\*\* $P < 0.001$ .

vascular development, were significantly regulated after 2 and 4 mg/L AgNP treatment in zebrafish embryos, indicating that these two signaling pathways may be involved in AgNP-induced neural and vascular developmental disruption in zebrafish.

Next, we summarized the DEGs enriched in the neuroactive ligand-receptor interaction pathway and the Vegf signaling pathway in AgNP-treated zebrafish at various concentrations (Figure 4C and D). Similar results were obtained using qPCR. In this context, the mRNA expression levels of *si:ch73-55i23.1*, *nfatc2a*, *rac1b*, *zgc:171775*, *kdr*, *prkcg*, *sh211-132p1.2*, *chrnb1*, *cckar*, *sstr2a*, *pla2g4aa*, *mapk1*, *p2ry6*, *adrb2a*, and *lpar4* decreased, whereas the expression levels of *prkcg*, *lepa*, *mchr1b*, and *chrmb1* significantly increased in zebrafish embryos after 72-h of exposure to 2 or 4 mg/L AgNP ( $P < 0.05$ ; Figure 4E and F). In addition, we used KOBAS software (version 3.0) to analyze the potential roles of these DEGs in neuroactive ligand-receptor interaction and Vegf signaling pathways. The results indicated that these DEGs were critically involved in regulating neuroactive ligand-receptor and Vegf signaling pathways (marked in red, Figure 5A and B), suggesting that AgNP exposure could impair several key regulatory factors of these two signaling pathways after 72 h of treatment in zebrafish embryos.

## Discussion

The widespread use of AgNP in production and daily necessities has caused extensive concern owing to its biologically toxic effects on human health, including developmental toxicity, teratogenicity, neurotoxicity, and vascular toxicity.<sup>5,12</sup> AgNP may enter the body orally, dermally and by inhalation.<sup>25</sup> Once AgNP enters the bloodstream, they are distributed throughout the body, including the central nervous system (CNS).<sup>25</sup> Previous studies reported that the function of the blood-brain barrier was impaired AgNP could in rats treated with Ag-NPs.<sup>26</sup> Exposure to AgNP may lead to vascular dysfunction.<sup>27</sup>

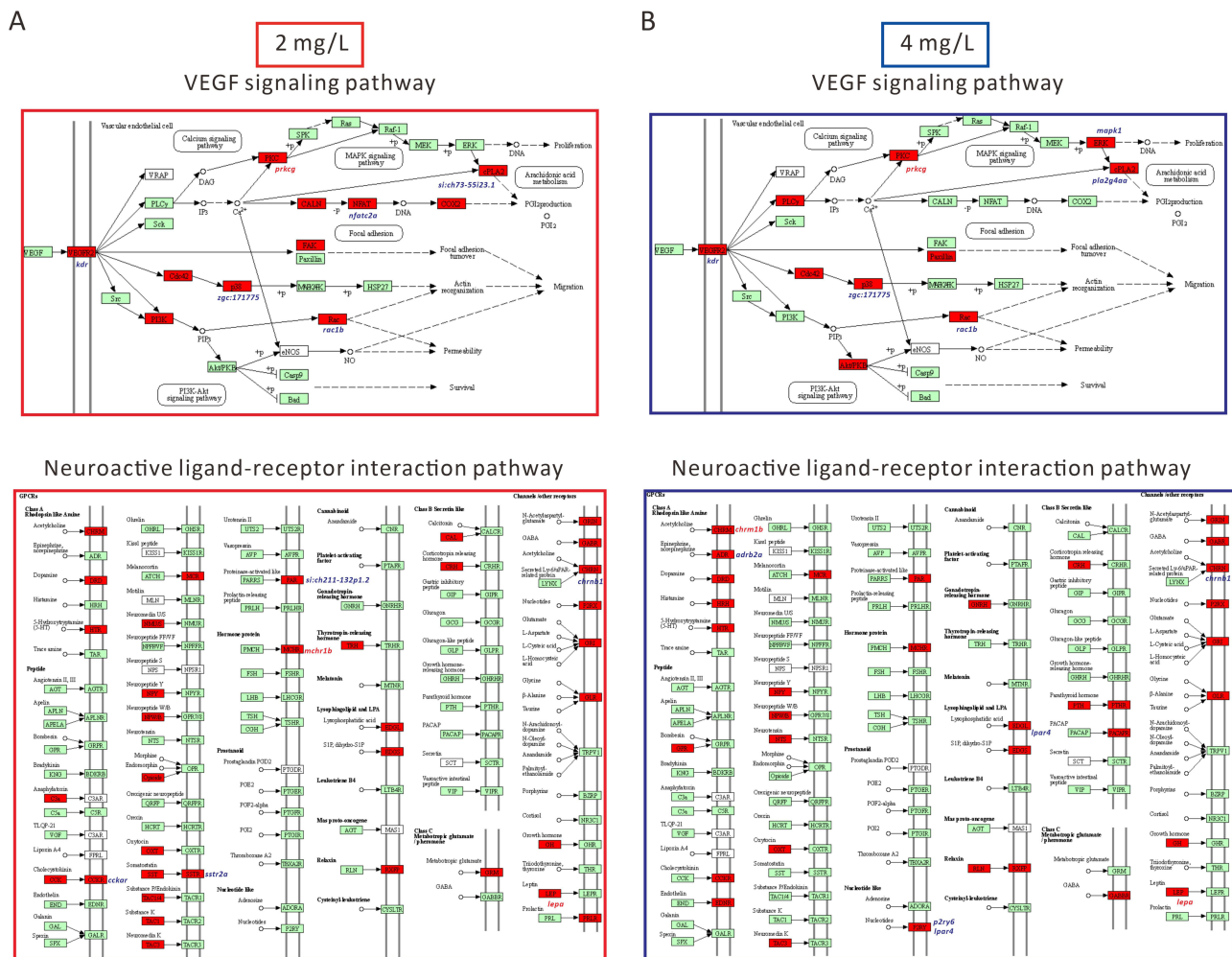


**Figure 5** Schematic representation of the DEGs of neuroactive ligand-receptor interaction and Vegf signaling pathway in zebrafish after 72 h of AgNP exposure at various concentrations. **(A)** DEGs diagram of neuroactive ligand-receptor interactions and Vegf signaling pathways after exposure to 2 mg/L AgNP. **(B)** DEGs diagram of neuroactive ligand-receptor interactions and Vegf signaling pathways after exposure to 4 mg/L AgNP. The red shading represents the DEGs in these two signaling pathways.

The particle size of AgNP is an essential factor affecting their toxicity. Previous studies demonstrated that 20–60 nm AgNP treatment would significantly increase the mortality rate at 4 mg/L,<sup>28</sup> and exposure to the smaller AgNP (6–14 nm) also significantly inhibit the survival rate and body length of zebrafish embryos at 5 mg/L concentration.<sup>29</sup> Similarly, 50 nm AgNP treatment at 1 mg/L would cause vascular toxicity at 24 hpf.<sup>5</sup> Most studies focus on the toxicity of AgNP at fixed particle size. However, the particle size of AgNP is not uniform in the human environment. Our previous study also found that AgNP treatment could significantly inhibit body length and cause developmental deformities in zebrafish embryos at 1 mg/L concentration.<sup>17</sup> In this study, we mainly analyzed the neural and vascular development in zebrafish under the combination of AgNP size of 10–100 nm.

Previous reports have indicated that AgNP can reduce neurite extension and branching, affecting neurogenesis in live cells.<sup>30</sup> In addition, AgNP can cause damage and dysfunction of HUVECs by inducing the oxidative stress response,<sup>31</sup> which may impair zebrafish embryos during the early developmental stage.<sup>32</sup> This study aimed to evaluate the neural and vascular developmental toxicity of AgNP and illustrate its regulatory mechanism in zebrafish embryos. The morphological determination revealed that AgNP exposure could impair neurological development, such as the “small eye” phenotype and the integrity of axon pattern, and subsequently result in motility dysfunction in zebrafish embryos (Figures 1 and 2). In addition, we found that AgNP exposure suppressed vascular development and induced vascular malformations in the zebrafish (Figure 3). Further RNA-seq analyses and qPCR revealed that neuroactive ligand-receptor and VEGF signaling pathways were significantly regulated after 72 h of AgNP exposure in zebrafish embryos (Figure 4),

implying that AgNP can lead to neural and vascular developmental toxicity by disturbing neuroactive ligand-receptor interactions and Vegf signaling pathways in zebrafish.

It has been reported that AgNP exposure can lead to death and delayed hatching in zebrafish,<sup>17,33</sup> implying that AgNP can damage organs and/or restrain development through different pathways. In the neural system, previous studies indicated that various degrees of developmental defects and abnormal phenotypes, such as small heads, small eyes, and cardiac defects, were induced by acute exposure to AgNP in zebrafish embryos.<sup>15</sup> Zhang et al found that AgNP exposure can lead to eye abnormalities by inhibiting lens development in zebrafish.<sup>34</sup> A recent report demonstrated that AgNP exposure exhibits developmental neurotoxic effects in pluripotent stem cell (PSC)-derived cerebral organoids.<sup>35</sup> Our results showed that AgNP affects eye development, and the eyes in the AgNP-treated group were statistically smaller than those in the control group after AgNP exposure (Figure 1), which is consistent with the concept of the eyeless phenotype induced by AgNP-treated zebrafish.<sup>36</sup> Moreover, our results demonstrated that neuronal morphology, including fluorescence intensity, motor neuron length, and locomotor behavior, were affected by AgNP exposure in fluorescence-labeled transgenic zebrafish (Figure 2).

AgNP can penetrate the cell membranes into internal tissues.<sup>37</sup> The micronuclei and nuclear abnormalities have also been observed in the peripheral blood cells of zebrafish,<sup>38</sup> suggesting that AgNP may play a mechanistic role in regulating signaling pathways in neural or vascular epithelial cells. Our KEGG pathway analyses identified that the neuroactive ligand-receptor interaction pathway was enriched in AgNP-treated zebrafish embryos (Figure 4), suggesting that AgNP may induce neurotoxicity by regulating the neuroactive ligand-receptor interaction pathway, which is consistent with a previous report that AgNP affects the neuroactive ligand-receptor interaction signaling pathway in the rat.<sup>39</sup> Neuroactive ligand-receptor interaction signaling pathway was closely related to neural function.<sup>40</sup> Disruption of genes associated with neuroactive ligand-receptor interactions affects memory function.<sup>41</sup> Further analyses using qPCR confirmed that several mRNA levels of key regulatory factors of the neuroactive ligand-receptor interaction signaling pathway, including *chrnb1*, *sstr2a*, *p2ry6*, *adrb2a*, *lpar4*, *lepa*, *mchr1b*, and *chrmlb*, which were also identified by RNA-seq analyses (Figure 4D), were statistically changed (Figure 4E and F). In addition, although not statistically significant, a trend towards regulated mRNA levels of *sh211-132p1.2* and *cckar* was observed in AgNP-treated zebrafish embryos (Figure 4E). Specifically, a previous study indicated that *CHRN1* encodes the  $\beta$ -subunit of the acetylcholine receptor (AChR) at the neuromuscular junction. The deletion of *CHRN1* results in an inherited neuromuscular disorder corresponding to the human congenital myasthenic syndrome.<sup>42</sup> The abnormal expression of somatostatin receptor 2 (SSTR2) is usually accompanied by neuroendocrine tumor and growth hormone-secreting pituitary adenoma.<sup>43</sup> Extracellular nucleotides exert their actions through two subfamilies of purine receptors: P2X and P2Y, and P2Y purinoceptor immunoreaction was seen in almost all ganglion cells.<sup>44</sup> *Chrn1* (cholinergic receptor, nicotinic, beta 1) contributes to acetylcholine receptor activity. In addition, *adrb2a* is also known as the gene encoding the  $\beta$ -adrenergic receptor in zebrafish, which is localized in the brain and involved in the oxidative stress response.<sup>45</sup> Our previous study also found that AgNP can induce oxidative stress in zebrafish.<sup>17</sup> Lysophosphatidic acid (LPA) was robustly expressed in migratory neurons, which depleted neurons show impaired multipolar-to-bipolar transition.<sup>46</sup> The *mchr1b* encodes a protein, the homologous protein of human MCHR1 (melanin-concentrating hormone receptor 1), and has been reported to be involved in the neuropeptide signaling pathway by modulating G protein-coupled receptor activity in vertebrates.<sup>47</sup> Leptin (Lep) plays an important role in regulating energy homeostasis in vertebrates,<sup>48</sup> and leptin also directly regulates kisspeptin neurons in the hypothalamus.<sup>49</sup> Recent studies indicated that the ortholog gene of *chrml1* (cholinergic receptor muscarinic 1), human *CHRM1* implicated in myasthenia gravis, Alzheimer's disease, Parkinson's disease, and frontotemporal dementia.<sup>50,51</sup>

Our results confirmed that AgNP exposure induced vascular malformation in zebrafish embryos (Figure 3) by regulating the Vegf signaling pathway (Figure 4). A previous study also demonstrated that AgNP might block VEGF-induced cell proliferation and migration in bovine retinal endothelial cells,<sup>52</sup> suggesting that AgNP exposure may be involved in angiogenesis. The VEGF signaling pathway, which contains VEGF and its receptor and their downstream signals, is the key angiogenic signaling pathway and promotes differentiation, proliferation, migration, sprouting, and angiogenic remodeling of endothelial cells.<sup>53</sup> The RNA-seq analyses and qPCR revealed that the overlapping regulated Vegf pathway-related genes, including *kdr*, *prkcg*, *rac1b*, and *zgc:171775*, were determined in AgNP-treated zebrafish embryos at various concentrations (Figure 4E and F). In this context, the KDR encoding protein, also known as VEGFR2, is the VEGF receptor and plays a critical role in the VEGF signaling pathway.<sup>54</sup> A previous report showed that *KDR* is essential for angiogenesis and collateral formation.<sup>55</sup> In addition, protein kinase C gamma (PKCgamma),

encoded by *PRKCG*, is a key downstream regulatory factor of the VEGF signaling pathway, which is also required for hypoxia-induced pathological retinal neovascularization through the activation of Src-phospholipase D1 (PLD1)-dependent PKC $\gamma$  signaling axis.<sup>56,57</sup> We also found that the mRNA levels of *kdr*, *prkeg*, *rac1b*, and *zgc:171775* were affected in zebrafish embryos after AgNP treatment. Previous studies demonstrated that the protein expression level of PRKCGA was up-regulated in patients with thyroid-associated ophthalmopathy,<sup>58</sup> and abnormal PKC regulation was associated with major depression.<sup>59</sup> Tan et al also found that Rac1 was essential for embryonic development because its endothelia-specific deletion led to an early embryonic lethal vascular phenotype.<sup>60</sup> Thus, we hypothesize that AgNP may lead to vascular developmental toxicity by regulating the Vegf signaling pathway-related genes in zebrafish embryos.

## Conclusion

In summary, our results showed that acute exposure to AgNP resulted in neural and vascular toxicity with detrimental effects on neuron maturation processes (axon formation) and angiogenesis in zebrafish embryos. Using in vitro experiments, we found that AgNP exposure inhibited lumen formation in HUVECs cells. In addition, transcriptome sequencing analyses and qRT-PCR indicated that the neuroactive ligand-receptor interaction pathway and Vegf signaling play important roles in AgNP-induced neurotoxicity and vascular toxicity, respectively. Our findings provide evidence to clarify the mechanism of neural and vascular toxicity caused by acute exposure to AgNP, which might reveal the potential risks that come along with AgNP exposure.

## Data Sharing Statement

The RNA-seq data have been deposited in the Sequence Read Archive of the National Center for Biotechnology Information under accession number PRJNA793391.

## Acknowledgments

This work was supported by the National Natural Science Foundation of China (81872070), Science and Technique Foundation of Guangdong Province (210728156901639), Natural Science Foundation of Guangdong Province (2022A1515012424), and Guangxi Natural Science Foundation for Guangdong - Guangxi United Program (2021GXNSFDA075014).

## Disclosure

The authors declare that they have no known competing financial interests or personal relationships that could have appeared to influence the work reported in this paper.

## References

1. Bao S, Tang W, Fang T. Sex-dependent and organ-specific toxicity of silver nanoparticles in livers and intestines of adult zebrafish. *Chemosphere*. 2020;249:126172. doi:10.1016/j.chemosphere.2020.126172
2. Stevenson LM, Dickson H, Klanjscek T, et al. Environmental Feedbacks and Engineered Nanoparticles: mitigation of Silver Nanoparticle Toxicity to *Chlamydomonas reinhardtii* by Algal-Produced Organic Compounds. *PLoS One*. 2013;8(9):e74456. doi:10.1371/journal.pone.0074456
3. Lyon TDB, Patriarca M, Howatson G, et al. Age dependence of potentially toxic elements (Sb, Cd, Pb, Ag) in human liver tissue from paediatric subjects. *J Environ Monit*. 2002;4:1034–1039.
4. Boyle D, Goss GG. Effects of silver nanoparticles in early life-stage zebrafish are associated with particle dissolution and the toxicity of soluble silver. *Nanoimpact*. 2018;12:1–8.
5. Gao J, Mahapatra CT, Mapes CD, et al. Vascular toxicity of silver nanoparticles to developing zebrafish (*Danio rerio*). *Nanotoxicology*. 2016;10:1363–1372.
6. Qiang L, Arabeyyat ZH, Xin Q, et al. Silver Nanoparticles in Zebrafish (*Danio rerio*) Embryos: uptake, Growth and Molecular Responses. *Int J Mol Sci*. 2020;21:1876.
7. Mosselhy D, He W, Li D, et al. Silver nanoparticles: in vivo toxicity in zebrafish embryos and a comparison to silver nitrate. *J Nanopart Res*. 2016;18:222.
8. McGillicuddy E, Murray I, Kavanagh S, et al. Silver nanoparticles in the environment: sources, detection and ecotoxicology. *Sci Total Environ*. 2017;575:231–246.
9. Campbell LA, Gormley PT, Bennett JC, et al. Functionalized silver nanoparticles depress aerobic metabolism in the absence of overt toxicity in brackish water killifish, *Fundulus heteroclitus*. *Aquat Toxicol*. 2019;213:105221.
10. Ma Y, Song L, Lei Y, et al. Sex dependent effects of silver nanoparticles on the zebrafish gut microbiota. *Environ Sci Nano*. 2018;5:704.
11. Rajkumar KS, Kanipandian N, Thirumurugan R. Toxicity assessment on haematology, biochemical and histopathological alterations of silver nanoparticles-exposed freshwater fish *Labeo rohita*. *Appl Nanosci*. 2016;6(1):19–29. doi:10.1007/s13204-015-0417-7

12. Powers CM, Slotkin TA, Seidler FJ, et al. Silver nanoparticles alter zebrafish development and larval behavior: distinct roles for particle size, coating and composition. *Neurotoxicol Teratol.* 2011;33(6):708–714. doi:10.1016/j.ntt.2011.02.002
13. Asharani PV, Wu Y, Gong Z, et al. Toxicity of silver nanoparticles in zebrafish models. *Nanotechnology.* 2008;19(25):255102. doi:10.1088/0957-4484/19/25/255102
14. Yeo MK, Yoon JW. Comparison of the Effects of Nano-silver Antibacterial Coatings and Silver Ions on Zebrafish Embryogenesis. *Mol Cell Toxicol.* 2009;5:23–31.
15. Xin Q, Rotchell JM, Cheng J, et al. Silver nanoparticles affect the neural development of zebrafish embryos. *J Appl Toxicol.* 2015;35(12):1481–1492. doi:10.1002/jat.3164
16. Jia H-R, Zhu Y-X, Xu K-F, et al. Efficient cell surface labelling of live zebrafish embryos: wash-free fluorescence imaging for cellular dynamics tracking and nanotoxicity evaluation. *Chem Sci.* 2019;10(14):4062–4068. doi:10.1039/C8SC04884C
17. Lu C, Lv Y, Kou G, et al. Silver nanoparticles induce developmental toxicity via oxidative stress and mitochondrial dysfunction in zebrafish (*Danio rerio*). *Ecotoxicol Environ Saf.* 2022;243:113993. doi:10.1016/j.ecoenv.2022.113993
18. Westerfield M. *The Zebrafish Book: A Guide for the Laboratory Use of Zebrafish (Danio Rerio)*. Eugene: University of Oregon Press; 2007.
19. Zhang J, Wang G, Huang A, et al. Association between Serum Level of Multiple Trace Elements and Esophageal Squamous Cell Carcinoma Risk: a Case–Control Study in China. *Cancers.* 2022;14(17):4239. doi:10.3390/cancers14174239
20. Bu D, Luo H, Huo P, et al. KOBAS-i: intelligent prioritization and exploratory visualization of biological functions for gene enrichment analysis. *Nucleic Acids Res.* 2021;49:W317–W325.
21. Jia P, Ma Y, Lu C, et al. The Effects of Disturbance on Hypothalamus-Pituitary-Thyroid (HPT) Axis in Zebrafish Larvae after Exposure to DEHP. *PLoS One.* 2016;11:e0155762.
22. Lu CJ, Jiang XF, Junaid M, et al. Graphene oxide nanosheets induce DNA damage and activate the base excision repair (BER) signaling pathway both in vitro and in vivo. *Chemosphere.* 2017;184:795–805.
23. Livak KJ, Schmittgen TD. Analysis of relative gene expression data using real-time quantitative PCR and the 2(-Delta Delta C(T)) method. *Methods.* 2001;25:402–408.
24. Yang XJ, Chen GL, Yu SC, et al. TGF-beta 1 enhances tumor-induced angiogenesis via JNK pathway and macrophage infiltration in an improved zebrafish embryo/xenograft glioma model. *Int Immunopharm.* 2013;15:191–198.
25. Liu F, Mahmood M, Xu Y, et al. Effects of silver nanoparticles on human and rat embryonic neural stem cells. *Front Neurosci.* 2015;9:115.
26. Sharma HS, Sharma A. Nanoparticles aggravate heat stress induced cognitive deficits, blood-brain barrier disruption, edema formation and brain pathology. *Prog Brain Res.* 2007;162:245–273.
27. Holland NA, Thompson LC, Vidanapathirana AK, et al. Impact of pulmonary exposure to gold core silver nanoparticles of different size and capping agents on cardiovascular injury. *Part Fibre Toxicol.* 2016;13(1):48.
28. Cunningham B, Engstrom AM, Harper BJ, et al. Silver Nanoparticles Stable to Oxidation and Silver Ion Release Show Size-Dependent Toxicity In Vivo. *Nanomaterials.* 2021;11(6):1516.
29. Lee CY, Horng JL, Chen PY, et al. Silver nanoparticle exposure impairs ion regulation in zebrafish embryos. *Aquat Toxicol.* 2019;214:105263.
30. Cooper RJ, Spitzer N. Silver nanoparticles at sublethal concentrations disrupt cytoskeleton and neurite dynamics in cultured adult neural stem cells. *Neurotoxicology.* 2015;48:231–238.
31. Shi J, Sun X, Lin Y, et al. Endothelial cell injury and dysfunction induced by silver nanoparticles through oxidative stress via IKK/KF-κB pathways. *Biomaterials.* 2014;35:6657–6666.
32. Chen G, Wang L, Li W, et al. Nodularin induced oxidative stress contributes to developmental toxicity in zebrafish embryos. *Ecotoxicol Environ Saf.* 2020;194:110444.
33. Christen V, Capelle M, Fent K. Silver nanoparticles induce endoplasmatic reticulum stress response in zebrafish. *Toxicol Appl Pharmacol.* 2013;272:519–528.
34. Zhang Y, Wang Z, Zhao G, et al. Silver nanoparticles affect lens rather than retina development in zebrafish embryos. *Ecotoxicol Environ Saf.* 2018;163:279–288.
35. Huang Y, Guo L, Cao C, et al. Silver nanoparticles exposure induces developmental neurotoxicity in hiPSC-derived cerebral organoids. *Sci Total Environ.* 2022;845:157047.
36. Lee KJ, Nallathamby PD, Browning LM, et al. In vivo imaging of transport and biocompatibility of single silver nanoparticles in early development of zebrafish embryos. *ACS Nano.* 2007;1:133–143.
37. Xiao B, Wang X, Yang J, et al. Bioaccumulation kinetics and tissue distribution of silver nanoparticles in zebrafish: the mechanisms and influence of natural organic matter. *Ecotoxicol Environ Saf.* 2020;194:110454.
38. Krishnaraj C, Harper SL, Yun SI. In vivo toxicological assessment of biologically synthesized silver nanoparticles in adult zebrafish (*Danio rerio*). *J Hazard Mater.* 2016;301:480–491.
39. Dan M, Wen H, Shao A, et al. Silver nanoparticle exposure induces neurotoxicity in the rat hippocampus without increasing the blood-brain barrier permeability. *J Biomed Nanotechnol.* 2018;14:1330–1338.
40. Wei J, Liu J, Liang S, et al. Low-Dose Exposure of Silica Nanoparticles Induces Neurotoxicity via Neuroactive Ligand-Receptor Interaction Signaling Pathway in Zebrafish Embryos. *Int J Nanomedicine.* 2020;15:4407–4415.
41. Papassotiropoulos A, de Quervain DJ. Failed drug discovery in psychiatry: time for human genome-guided solutions. *Trends Cogn Sci.* 2015;19(4):183–187.
42. Freed AS, Schwarz AC, Brei BK, et al. CHRNB1-associated congenital myasthenia syndrome: expanding the clinical spectrum. *Am J Med Genet A.* 2021;185:827–835.
43. Steven AK, Kayser A, Wetz C, et al. Somatostatin analogues in the treatment of neuroendocrine tumors: past, present and future. *Int J Mol Sci.* 2019;20:3049.
44. Zhang PP, Yang XL, Zhong YM. Cellular localization of P2Y<sub>6</sub> receptor in rat retina. *Neuroscience.* 2012;220:62–69.
45. Sun L, Liu F, Chen H, et al. Transcriptional responses in adult zebrafish (*Danio rerio*) exposed to propranolol and metoprolol. *Ecotoxicology.* 2015;24:1352–1361.
46. Kurabayashi N, Tanaka A, Nguyen MD, et al. The LPA-LPA4 axis is required for establishment of bipolar morphology and radial migration of newborn cortical neurons. *Development.* 2018;145(17):dev162529.

47. Bächner D, Kreienkamp HJ, Richter D. MIZIP, a highly conserved, vertebrate specific melanin-concentrating hormone receptor 1 interacting zinc-finger protein. *FEBS Lett.* 2002;526:124–128.
48. Wang B, Cui A, Wang P, et al. Temporal expression profiles of leptin and its receptor genes during early development and ovarian maturation of *Cynoglossus semilaevis*. *Fish Physiol Biochem.* 2020;46(1):359–370.
49. Ohga H, Hirata D, Matsumori K, et al. Possible role of the leptin system in controlling puberty in the male chub mackerel, *Scomber japonicus*. *Comp Biochem Physiol A Mol Integr Physiol.* 2017;203:159–166.
50. Fang P, Yu C, Liu J, et al. Study on the potential mechanism of *Semen Strychni* against myasthenia gravis based on network pharmacology and molecular docking with experimental verification. *Evid Based Complement Alternat Med.* 2022;2022:3056802.
51. Sabbir MG, Speth RC, Albensi BC. Loss of cholinergic receptor muscarinic 1 (CHRM1) protein in the hippocampus and temporal cortex of a subset of individuals with Alzheimer's disease, Parkinson's disease, or frontotemporal dementia: implications for patient survival. *J Alzheimers Dis.* 2022;90:727–747.
52. Kalishwaralal K, Banumathi E, Pandian SRK, et al. Silver nanoparticles inhibit VEGF induced cell proliferation and migration in bovine retinal endothelial cells. *Colloid Surf B Biointerfaces.* 2009;73:51–57.
53. Evans I. An overview of VEGF-mediated signal transduction. *Methods Mol Biol.* 2015;1332:91–120.
54. Shibuya M. Vascular endothelial growth factor and its receptor system: physiological functions in angiogenesis and pathological roles in various diseases. *J Biochem.* 2013;153:13–19.
55. Ylä-Herttua S, Rissanen TT, Vajanto I, et al. Vascular endothelial growth factors: biology and current status of clinical applications in cardiovascular medicine. *J Am Coll Cardiol.* 2007;49:1015–1026.
56. Zhang Q, Wang D, Kundumani-Sridharan V, et al. PLD1-dependent PKC $\gamma$  activation downstream to Src is essential for the development of pathologic retinal neovascularization. *Blood.* 2010;116:1377–1385.
57. Zhang Q, Wang D, Singh NK, et al. Activation of cytosolic phospholipase A2 downstream of the Src-phospholipase D1 (PLD1)-protein kinase C  $\gamma$  (PKC $\gamma$ ) signaling axis is required for hypoxia-induced pathological retinal angiogenesis. *J Biol Chem.* 2011;286:22489–22498.
58. Wang Y, Shao Y, Zhang H, et al. Comprehensive analysis of key genes and pathways for biological and clinical implications in thyroid-associated ophthalmopathy. *BMC Genomics.* 2022;23(1):630.
59. Abrial E, Etievant A, Bétry C, et al. Protein kinase C regulates mood-related behaviors and adult hippocampal cell proliferation in rats. *Prog Neuropsychopharmacol Biol Psychiatry.* 2013;43:40–48.
60. Tan W, Palmby TR, Gavard J, et al. An essential role for Rac1 in endothelial cell function and vascular development. *FASEB J.* 2008;22(6):1829–1838.

International Journal of Nanomedicine

Dovepress

## Publish your work in this journal

The International Journal of Nanomedicine is an international, peer-reviewed journal focusing on the application of nanotechnology in diagnostics, therapeutics, and drug delivery systems throughout the biomedical field. This journal is indexed on PubMed Central, MedLine, CAS, SciSearch<sup>®</sup>, Current Contents<sup>®</sup>/Clinical Medicine, Journal Citation Reports/Science Edition, EMBase, Scopus and the Elsevier Bibliographic databases. The manuscript management system is completely online and includes a very quick and fair peer-review system, which is all easy to use. Visit <http://www.dovepress.com/testimonials.php> to read real quotes from published authors.

Submit your manuscript here: <https://www.dovepress.com/international-journal-of-nanomedicine-journal>